JCTC Journal of Chemical Theory and Computation

Ab Initio Molecular Dynamics Study of Mg^{2+} and Ca^{2+} Ions in Liquid Methanol

Cristian Faralli,[†] Marco Pagliai,[†] Gianni Cardini*[,†,‡] Vincenzo Schettino[†,‡]

Laboratorio di Spettroscopia Molecolare, Dipartimento di Chimica, Università di Firenze, Via della Lastruccia 3, 50019 Sesto Fiorentino, Firenze, Italia, and European Laboratory for Nonlinear Spectroscopy (LENS), via Nello Carrara 1, 50019 Sesto Fiorentino, Firenze, Italia

Received August 22, 2007

Abstract: Ab initio Car−Parrinello molecular dynamics simulations have been performed in order to investigate the solvation properties of Mg^{2+} and Ca^{2+} in fully deuterated methanol solution to better understand polarization effects induced by the ions. Charge transfer and dipole moment calculations have been performed to give more detailed insight on the role of the electronic reorganization and its effect on the first solvation shell stability. The perturbation of the methanol H-bond network has been investigated.

Introduction

Simulation studies of the structural and dynamical properties of solutions of ions in polar solvents are of great importance to understand the effects of charged species on the physical and chemical properties of ionic solutions. The presence of ions can strongly perturb the structure of the liquid, and this can have relevant effects on the chemical reactivity in solution. In general a particular role is played by the stability of the first solvation shell although in some cases the perturbation extends farther away from the ion. Despite the large variety of polar solvents of common use in chemistry, only water[1−11] and, to a lower extent, ammonia[4,12,13] have been extensively analyzed from the theoretical and computational point of view. A series of ab initio molecular dynamics and cluster calculations on ions in these solvents[14−20] has been performed showing the importance of polarization interactions in the reproduction of the experimental results.[1,21−24]

At present, methanol, the smallest molecule characterized by both a hydrophobic and a hydrophilic group, is widely used as a solvent, but the number of computational studies on the structural and dynamical properties of the liquid[7,21−29] and its ionic solutions[30−37] is limited. In the past few years the interest on methanol has also grown as a possible fuel cell component.[38−42] Therefore, the comprehension of the liquid methanol properties and its interactions with ions and simple molecules is becoming of paramount importance.

In this paper, we report on ab initio molecular dynamics simulations, within the Car−Parrinello (CPMD)[43−46] formalism, of Mg^{2+} and Ca^{2+} ions in methanol. Particular attention has been paid to the structure of the first solvation shell and to the change of ground-state electronic properties of the ions and of the solvent molecules. This kind of approach has been used with success to study ions in solution[16,30,31,47−59] showing that the most relevant effects are concerned with the first solvation shell. The nature of the interactions that stabilize the first solvation shell of the Mg^{2+} and Ca^{2+} ions in methanol has been interpreted in terms of charge transfer and polarization, confirming the stabilization model proposed in the case of the Li^+,[30] Na^+, and K^+ ions[31] in the same solvent.

Computational Details

The simulations have been performed with the CPMD code[43,46] in cubic boxes of 12.05 Å and 13.99 Å side with periodic boundary conditions using 25 and 40 methanol molecules, respectively, and one ion. The initial configuration with 25 molecules sample has been constructed starting from the last configuration extracted from a previous Car−Parrinello simulation of Li^+ in methanol[30] with the simple ion substitution. The initial configurations for the larger systems have been taken from the last configuration obtained performing a preliminary classical simulation (>100 ps)

* Corresponding author e-mail: gianni.cardini@unifi.it.
[†] Università di Firenze,.
[‡] European Laboratory for Nonlinear Spectroscopy (LENS).

10.1021/ct700209v CCC: $40.75
Published on Web 12/18/2007

using semiempirical potentials with Lennard-Jones parameters taken from the literature.[60]

After a thermalization at 300 K by velocity scaling (∼1 ps), the equations of motions have been integrated with a time step of 5 au (∼0.12 fs) in the NVE ensemble storing atomic coordinates and velocities for the subsequent analysis. The simulation time has been of ∼16 ps and ∼9 ps for Mg^{2+} and Ca^{2+}, respectively, in the 25 solvent molecules samples and of ∼11 ps for the samples with 40 methanol molecules. The computational protocol adopted in previous works[30,31,58] has shown that the time scale is sufficient to accurately reproduce the structural properties. The correct conservation of the energy, a sensitive parameter in CPMD charged systems, has been monitored during the whole simulation run.

Most of the analysis reported here have been performed on trajectories from simulations of the larger samples.

The deuterium has been used instead of hydrogen to allow for a larger time step. Density functional calculations in the generalized gradient approximation (GGA) have been performed using the BLYP[61,62] exchange correlation functional. A ficticious electronic mass of 800 au has been adopted to keep the system on the Born−Oppenheimer surface. The plane wave (PW) expansion has been truncated at 70 Ry.

Martins-Troullier[63] pseudopotentials (MT) have been used along with the Kleinman-Bylander[64] decomposition for the C, H, and O atomic species. For the calcium ion preliminary simulations with 25 methanol molecules have been performed adopting either a MT semicore pseudopotential (considering as core the 1s, 2s, and 2p electrons) or a Goedecker semicore pseudopotential (SG)[65,66] in order to analyze possible effects of the pseudopotential choice. The results of the two simulations showed very similar structural properties as reported in the Supporting Information (Figure 1-S). In the larger samples, for both calcium and magnesium ions, Goedecker[65,66] type pseudopotentials have been adopted as in previous works on monovalent cations in methanol.[30,31]

The reliability of the pseudopotentials and of the computational approach chosen for the simulations and the subsequent analysis has been confirmed by the convergence of the structural data with plane waves cutoff as reported in Table I-S of the Supporting Information. A good binding energy[67] convergence at 70 Ry has been obtained. Considering the higher extension of the basis set used in this work with respect to those present in literature,[68] adopting the B3LYP/6-31+G* level of theory calculations, the agreement with the literature values is fairly good. The "all electrons" calculations show a lower binding energy value for Mg^{2+} with respect to PWs expansion, with an opposite trend for Ca^{2+}, but in both cases the differences are lower than 2 kcal mol^{-1}.

Atoms in molecules (AIM)[69−71] and maximally localized Wannier function centers (WFCs) analysis[72,73] have been performed averaging over equi-spaced configurations in the samples with 40 methanol molecules, every 0.08 ps for Mg^{2+} and 0.09 ps for Ca^{2+}.

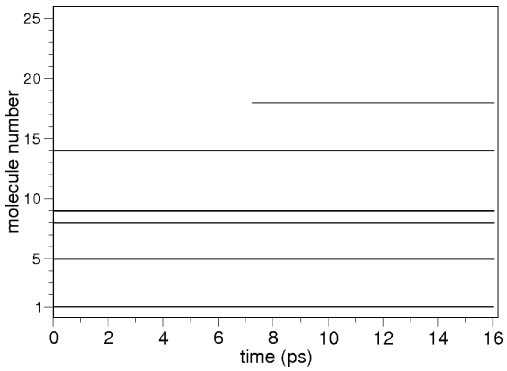

Figure 1. A dot is reported at each time step for a molecule in the first solvation shell.

Results and Discussion

The systems have been initially simulated in samples with 25 methanol molecules. In the case of the Mg^{2+} a peculiar behavior has been noticed. A 5-fold coordination has been observed during the initial 7.3 ps of the run (see Figure 1) with a square pyramidal basis coordination geometry (see Figure 2a). Subsequently the number of methanol molecules around the ion rises up abruptly to a stable 6-fold octahedral coordination (Figures 1 and 2b).

In order to explain this behavior, the energy of the optimized geometry for the two configurations (extracted before and after the coordination number change) has been computed for isolated clusters with "all electrons" calculations, using the BLYP functional and the 3-21+G** basis set. The clusters coordinates are reported in Tables II-S and III-S of the Supporting Information, and the first shell configurations are shown in Figure 2a,b. The results show a higher stability of the 6-fold coordinated cluster with a difference in the binding energy of 29.95 kJ mol^{-1}. This value is about 1 order of magnitude higher than the thermal energy at 300 K (2.49 kJ mol^{-1}) and explains the observed stability of the 6-fold coordinated ion once it is formed. The initial 5-fold configuration can be attributed to the selected starting configuration and to a likely too short thermalization run (∼1 ps) with respect to the cage relaxation time.

It is interesting to note that the salient structural data for the two parts of the simulation are not particularly different, as in Figure 2-S of the Supporting Information. In particular, comparison of the two partial pair distribution functions with the total shows that the first peak position is not appreciably affected by the variation of the coordination number.

In Figure 3 the pair radial distribution function for the Mg−O and Ca−O distances, together with their integration number, are reported for samples with 40 methanol molecules and compared with the system containing 25 solvent molecules.

It is evident that, for both ions, the sample dimension only affects the second solvation shell that is slightly better defined in the larger sample, showing clearly that it is formed by 6 molecules. In the case of Ca^{2+} a small effect on the height and width of the first peak can also be noted implying a greater rigidity of the first solvation shell in the smaller simulation box. The stability of the second shell is higher for the larger samples as it can be inferred from the slightly deeper second minimum.

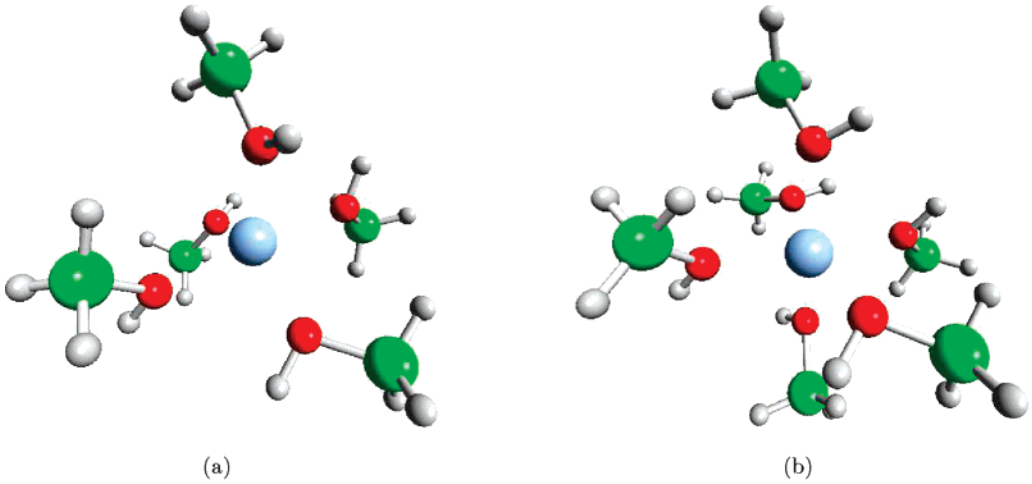

Figure 2. Mg ion and its nearest neighbors: (a) configuration extracted from the first part of simulation (pentacoordination) and (b) configuration referred to the second part of simulation.

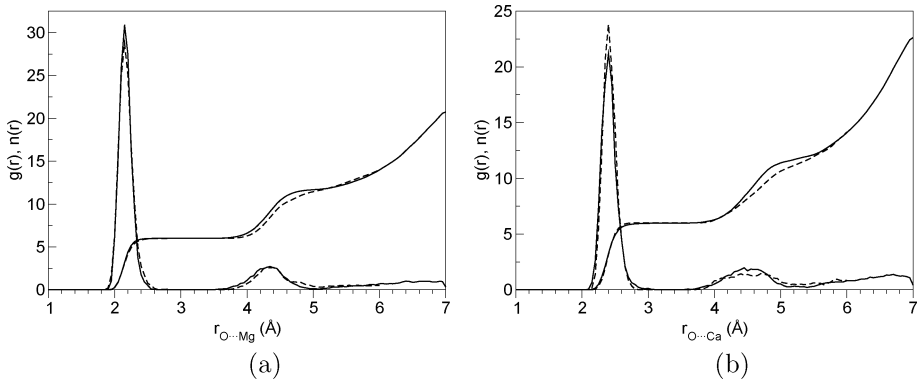

Figure 3. Pair radial distribution functions and integration numbers of Mg^{2+} (a) and Ca^{2+} (b) with 25 methanol molecules (dashed lines) and with 40 methanol molecules (full lines), respectively.

Table 1. Salient Structural Data (Distances in Å) for Mg^{2+} and Ca^{2+} Solutions with 25 and 40 Solvent Molecules[a]

	O···M^{2+}	cutoff	*n*(*r*)
Mg^{2+} (25)	2.15	3.00	5.6 (5 or 6)
Mg^{2+} (40)	2.15	3.00	6.0
Radnai et al.[74]	2.068		5.95
Tamura et al.[75]	2.00	2.5−3	6.0
Ca^{2+} (25)	2.40	3.25	6.0
Ca^{2+} (40)	2.40	3.45	6.0
Megyes et al.[76,77]	2.39		6.0

[a] The coordination number, *n*(*r*), has been computed at the cutoff distance. The data are compared with experimental results.

Table 1 reports the position of the first peak in the radial distribution function and the integration number.

It can be seen that the cutoff distance has no effect on the coordination number due to the fact that the first minimum in the *g*(*r*) is widespread. X-ray diffraction studies[74] locate the first peak position at 2.068 Å with a "relatively rigid octahedral" cage thus proposing a 6-fold coordination. Subsequent studies, supported by molecular dynamics simulations,[75] confirmed these findings although with a first peak position at shorter distance (2.00 Å) than the X-ray result. In the present calculation the first peak position for Mg^{2+} solutions is found at a slightly larger distance (2.15 Å). The results of the present simulation are in full agreement with experiments[76,77] in the case of the Ca^{2+} ion.

For both ions the residence time of the methanol molecules in the first solvation shell is longer than the simulation time, and no exchange of methanol molecules has been observed between the first and second solvation shell, as can also be argued by the flat and deep minimum in the pair radial distribution functions. A similar behavior has been reported for water solution where many of these dications are surrounded by a rigid first solvation shell that shows a slow exchange of water molecules with the second shell.[14,15,78−80] Earlier, diffusion coefficient calculations and solvation simulations reported a very long lifetime for water molecules in the first solvation shell around Mg^{2+}, falling in the range of hundreds of picoseconds.[81,82]

The small amplitude of motion in the cage is well evident from the pair distribution functions (Figure 3) characterized by a very sharp first peak. This is further emphasized by the angular distribution function reported in Figure 3a-S along with the spatial distribution function[83−86] of Figure 3b-S obtained from the configurational space spanned by the ion considering a methanol molecule of the first solvation shell as the reference system. As expected, the oxygen lone pairs of the methanol molecules are steadily oriented in the

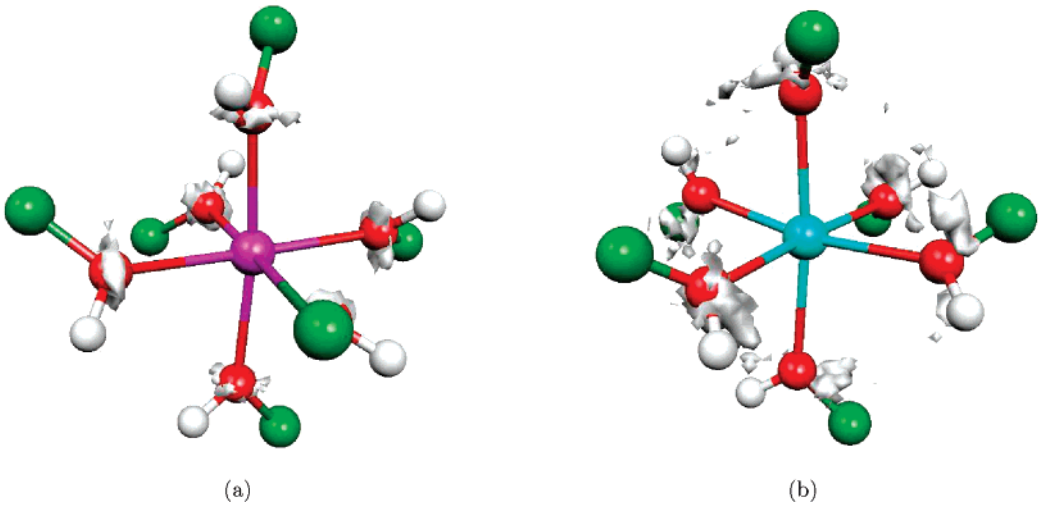

Figure 4. Spatial distribution functions for the first solvation shell of Mg^{2+} (a) and Ca^{2+} (b) in the system with 40 methanol molecules. The isosurface represents the 13% and the 16% of the maximum value for Mg^{2+} and Ca^{2+}, respectively. The methyl groups have been represented by the green spheres.

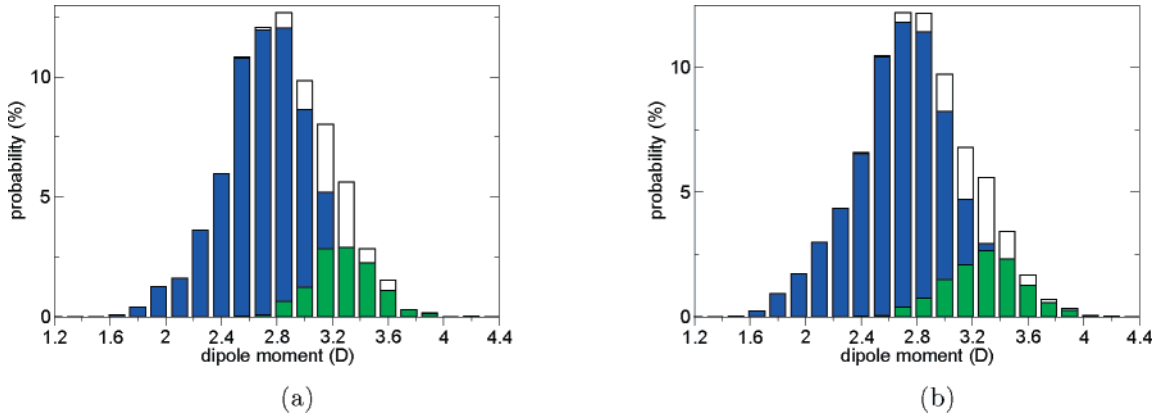

Figure 5. Dipole moment for methanol molecules with Mg^{2+} (a) and Ca^{2+} (b). The green bars refer to the dipole moment of the first shell molecules, whereas the blue bars describe the external molecules contribution. The average dipole moment of the whole solution is represented by the white bars.

Table 2. Average Dipole Moment Values (in Debye, D) and Relative Standard Deviation for the Solution ($<\mu>_{tot}$), for the First Shell Molecules Contribution ($<\mu>_{fs}$), and for the External Molecules ($<\mu>_{ext}$)

	$<\mu>_{tot}$	$<\mu>_{fs}$	$<\mu>_{ext}$
Mg^{2+} 25	2.9 ± 0.4	3.4 ± 0.4	2.7 ± 0.3
Mg^{2+} 40	2.8 ± 0.4	3.3 ± 0.2	2.7 ± 0.3
Ca^{2+} 25	2.8 ± 0.4	3.2 ± 0.3	2.7 ± 0.3
Ca^{2+} 40	2.8 ± 0.4	3.3 ± 0.3	2.7 ± 0.4

direction of Ca^{2+} with the COCa and HOCa tilt angles around 120° and 127°, respectively, with a small amplitude of motion around the ion.

To better characterize the structure of the cage in the larger sample salient average distances and angles are reported in Table IV-S. A pictorial view of the first solvation shell is shown in Figure 4 where the motion amplitude of the oxygen atoms around the ion is displayed. The spanned configurational space is found to be strictly localized around the vertices of an octahedron, particularly for Mg^{2+}, as can also be argued from the lower dispersion of the data.

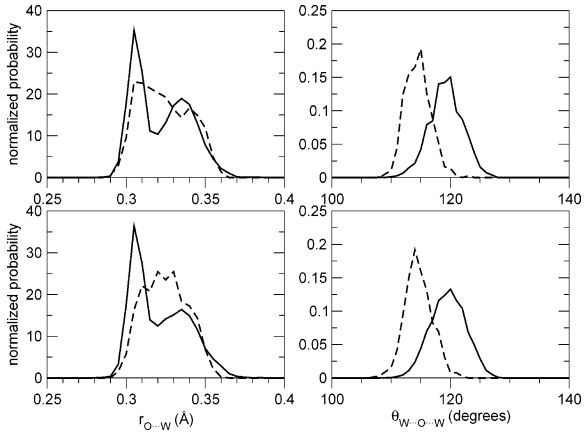

Figure 6. Radial distribution function of the oxygen-WFCs average distance ($r_{O\cdots W}$) and angular distribution function of the angle between the WFCs ($\theta_{W\cdots O\cdots W}$) for Mg^{2+} with 40 methanol molecules (top) and for Ca^{2+} with 40 methanol molecules (bottom). The dashed lines refer to the first shell molecules contribution.

The perturbation on the solvent structure, due to the presence of the ion, has been evaluated in terms of electronic

Table 3. Hydrogen Bond Network Characterization[a]

	Mg^{2+}		Ca^{2+}			Mg^{2+}		Ca^{2+}	
	fs	tot	fs	tot		fs	tot	fs	tot
f_0	100	18	100	22	g_0	100	1	99	3
f_1	0	67	0	62	g_1	0	18	1	23
f_2	0	15	0	16	g_2	0	65	0	58
f_3					g_3	0	16	0	16
$<n_f>$	0.00	0.98	0.00	0.94	$<n_g>$	0.00	1.95	0.01	1.85

[a] f_i represents the percentage of methanol molecules whose oxygen atom is involved in i H-bonds, and $<n_f>$ is the average number of received H-bonds per molecule; g_i is the percentage of methanol molecules that totally form i H-bonds, and $<n_g>$ is the average number of total H-bonds per molecule. The first shell (fs) molecules contribution has been put into evidence.

properties that illustrate the differences from the pure solvent.[25] The polarization effects are evidenced by the dipole moment computed through the maximally localized WFCs and shown in Figure 5.

The ion perturbation mainly affects the neighboring molecules that are highly polarized as it is seen from the change of the average total dipole moment ($\Delta\mu \sim 0.4$ D). In turn the dipole moment of the outer molecules approaches the value of the pure liquid (2.6 D)[25] remarking the weaker perturbation at long range. These results are summarized in Table 2 where it can be noted that the contribution to the dipole moment does not depend on the system size. In a recent paper,[31] the polarization provided by monovalent cations on the surrounding methanol molecules was found weaker. The stronger polarization due to these divalent cations with respect to monovalent ones has been also reported in water solution.[59]

For alkaline ions the size of the ions increases going from Li^+ to K^+, and, consequently, as expected, the induced dipole moment of the solvent molecules decreases. This is particularly evident for the first solvation shell molecules.[31] For magnesium and calcium ions a different trend can be observed: the longer O−Ca distance does not yield a weaker polarization effect with respect to magnesium ion, and the perturbation on the dipole moment values is similar for both ions.

Radial $r_{O\cdots W}$ and angular $\theta_{W\cdots O\cdots W}$ distributions of the WFCs of the oxygen lone pairs have been investigated to better understand the increase of the dipole moment of the first solvation shell molecules.[87] These are reported in Figure 6 showing separately the contribution of the first solvation shell molecules.

A different shape in the distribution of the $r_{O\cdots W}$ distances and a lower value in the $\theta_{W\cdots O\cdots W}$ angles are observed for the first shell molecules, whereas no change occurs between the oxygen and the WFCs attributed to the O−H and O−C covalent bonds (not reported). For the $\theta_{W\cdots O\cdots W}$ angle a smaller value can be observed for the lone-pair WFCs of the first shell molecules both in methanol and water solution,[16,50,87,88] while a different behavior is present in the $r_{O\cdots W}$ distance in the two solvents. A double peak in the distribution of $r_{O\cdots W}$ is found for the external molecules in methanol, while a symmetrical distribution has been found for the molecules directly solvating the ion. In the bulk, where no coordinative constrain is imposed, some methanol molecules are directionally H-bonded[25] through a single WFC. The methanol H-bonded lone pairs are less contracted on the oxygen than the noninteracting lone pairs providing a splitting of the peak. No H-bond network is permitted between the molecules of the first solvation shell. This can be attributed to the steric hindrance of the CH_3 group. The first shell methanol molecules interact with the ion through both the WFCs that are therefore not anymore available to accept hydrogen atoms from other methanol molecules. This is summarized in Table 3 (left panel) where the percentage of solvent molecules that accept H-bond formation, via oxygen atom, is reported along with the average number of accepted H-bonds per molecule. It can be noticed that no methanol molecule in the first solvation shell is a H-bond acceptor.

The table also reports (right panel) the distribution of the total hydrogen bonds in the system, showing that the majority of methanol molecules are involved in two hydrogen bonds, a result in agreement with finding in the pure solvent.[25,89,90]

Further insight on the solvent reorganization produced by the ion is obtained considering the angle θ_μ between the dipole moment vector ($\vec{\mu}$) and the oxygen-ion interaction axis (see Figure 7).[75,91]

It can be seen from the figure that for the first shell molecules θ_μ is quite tightly peaked around 18°, indicating a rigid structure of the solvation shell. For the outer molecules the distribution is very shallow. A similar behavior has been generally observed in water solutions[47,49,59,92−95] and only rarely in other solvents.[32] This behavior can be further enlightened considering the variation of the dipole moment orientation and its standard deviation as a function of the distance from the central ion (Figure 8).[75,91−93]

Neglecting the 3−4 Å range, where the statistics are rather poor, it can be seen that, up to 5 Å, θ_μ increases smoothly, and the deviations from the average value are small implying that there is a preferential orientation of the dipoles in the first and even in the second shell. Above 5 Å a higher disorder in the bulk of the solution is evident. Similar results have been obtained for Mg^{2+} (see Figure 5-S).

The charge-transfer analysis on the ions has been performed using the AIM approach proposed by Bader.[70] This method also allows the evaluation of the amount of the charge transfer as a function of the distance between the ion and the surrounding solvent molecules as it is depicted for Mg^{2+} with 40 methanol molecules in Figure 9.

The electronic charge transfer on the ions is 0.221 ± 0.003 e^- for Mg^{2+} and 0.347 ± 0.008 e^- for Ca^{2+}. The same trend was also observed in water solutions.[59] A smaller electronic

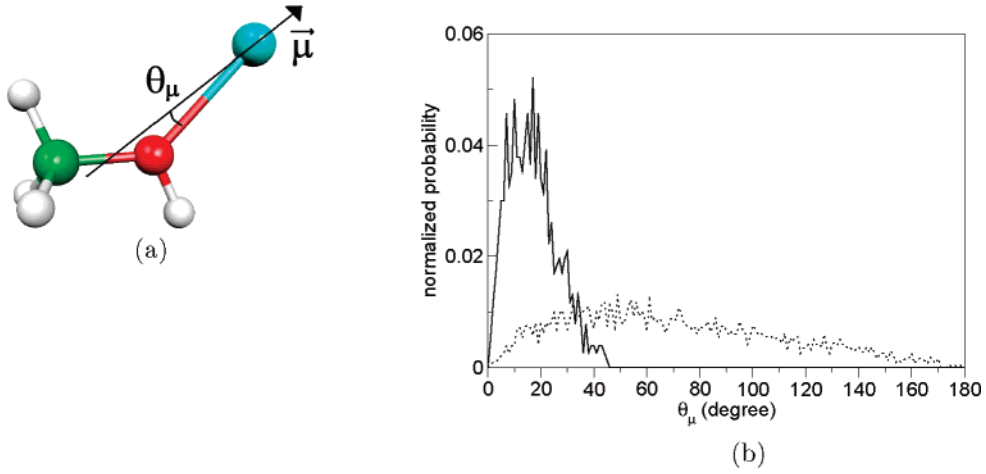

Figure 7. (a) Definition of the θ_μ angle between the dipole vector ($\vec{\mu}$) direction of the methanol molecules and the Ca−O axis. (b) Distribution function of θ_μ for the system with 40 molecules. The full line refers to the first shell contribution. The dotted line represents all other external molecule.

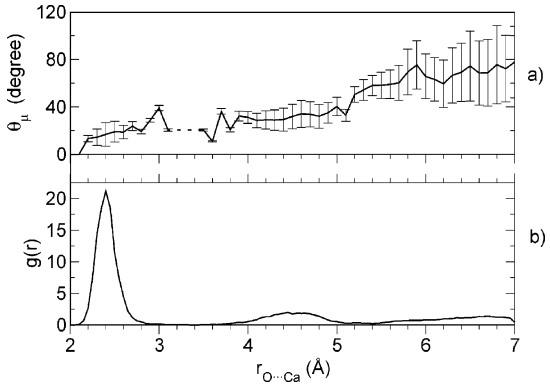

Figure 8. (a) Standard deviation on the average value of the θ_μ angle as a function of the distance from the calcium ion in the system with 40 methanol molecules. (b) O−Ca pair distribution function (same as Figure 3b with full lines).

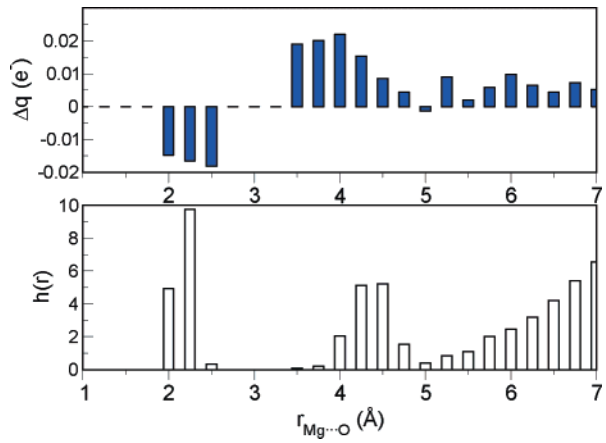

Figure 9. Charge-transfer distribution $\Delta q(e^-)$ as a function of the distance to the ion (upper panel) and not normalized O−Mg distribution function (lower panel) for Mg^{2+} with 40 methanol molecules.

displacement was observed for alkali metal cations together with a weaker polarization effect on the first shell molecules.[30,31] The higher value for the calcium ion is due to its greater softness with respect to magnesium as expected in going down along the group in the periodic table.[96] The same number of valence shell electrons and the same charge on Mg^{2+} and Ca^{2+} are distributed in a different atomic volume. The higher ionic radius[97,98] of Ca^{2+} implies a difference in hardness,[99,100] namely the resistance of the chemical potential to change the number of electrons.[96] Ca^{2+} can receive a greater charge amount from the first shell molecules that become very positively charged. The charge transfer from the second shell to the first is not sufficient to balance the charge transferred from the methanol molecules of the first solvation shell to the ion.

Conclusions

Ab initio CPMD calculations have been performed on solutions of methanol with Mg^{2+} and Ca^{2+} in order to investigate the reorganization effects on a protic solvent due to the presence of charged species. The reliability of the method has been stated by comparison with "all electrons" calculations with a localized Gaussian basis set, showing good agreement in the ion−methanol interaction. The first solvation shell properties have been analyzed and compared to the bulk solvent molecules. The structure of the solvent has been investigated using distribution functions and the electronic properties through the AIM population analysis and the maximally localized WFCs. The box size effects have been explored, and no evident consequence has been found on the first solvation shell.

Similar structural and electronic reorganization is induced on the solvent by the two ions. A stable octahedral coordination and a high polarization effect on the molecules of the first solvation shell have been observed. Analysis of the dipole moment vector has shown a preferential orientation up to 5 Å far from the Ca^{2+} with an influence on the organization of the second shell molecules as well. The characterization of the hydrogen bond network has shown a different trend with respect to that observed in water solution[16,50,87,88] without any solvent molecule in the first solvation shell behaving as a H-bond acceptor. Electronic charge-transfer analysis has confirmed the stabilization of the first solvation shell due to electrostatic interactions as discussed in the literature.[30,31]

Acknowledgment. This work has been supported by the Ministero dell'Istruzione, dell'Università e della Ricerca Scientifica (MIUR).

Supporting Information Available: Pair radial distribution function and an octahedral rearrangement of the cage around the ion (Figure 1-S), structural parameters for methanol−Mg^{2+} and methanol−Ca^{2+} clusters (Table I-S), Cartesian coordinates (Tables II-S and III-S), MgO pair radial distribution function and its running integration numbers for all the runs (Figure 2-S), angular and spatial distribution functions (Figure 3-S), structural parameters (Table IV-S and Figure 4-S), and standard deviation on the average value of the θ_μ (Figure 5-S).This material is available free of charge via the Internet at http://pubs.acs.org.

References

(1) Kuo, I.-F. W.; Mundy, C. J.; McGrath, M. J.; Siepmann, J. I.; VandeVondele, J.; Sprik, M.; Hutter, J.; Chen, B.; Klein, M. L.; Mohamed, F.; Krack, M.; Parrinello, M. *J. Chem. Phys. B* **2004**, *108*, 12990−12998.

(2) Lee, H.-S.; Tuckerman, M. E. *J. Chem. Phys.* **2007**, *126*, 164501.

(3) Todorova, T.; Seitsonen, A. P.; Hutter, J.; Kuo, I.-F. W.; Mundy, C. J. *J. Phys. Chem. B* **2006**, *110*, 3685−3691.

(4) Liu, Y.; Tuckerman, M. E. *J. Phys. Chem. B* **2001**, *105*, 6598−6610.

(5) Silvestrelli, P. L.; Parrinello, M. *Phys. Rev. Lett.* **1999**, *82*, 3308−3311.

(6) Silvestrelli, P.; Parrinello, M. *J. Chem. Phys.* **1999**, *111*, 3572−3580.

(7) Ladanyi, B. M.; Skaf, M. S. *Ann. Rev. Phys. Chem.* **1993**, *44*, 335−368.

(8) Gubskaya, A. V.; Kusalik, P. *J. Chem. Phys.* **2002**, *117*, 5290−5302.

(9) Luzar, A.; Chandler, D. *Phys. Rev. Lett.* **1996**, *76*, 928−931.

(10) Guillot, B. *J. Mol. Liq.* **2002**, *101*, 219−260.

(11) Jorgensen, W. L.; Chandrasekhar, J.; Madura, J. D.; Impey, R. W.; Klein, M. L. *J. Chem. Phys.* **1983**, *79*, 926−935.

(12) Boese, A. D.; Chandra, A.; Martin, J. M. L.; Marx, D. *J. Chem. Phys.* **2003**, *119*, 5965−5980.

(13) Diraison, M.; Martyna, G. J.; Tuckerman, M. E. *J. Chem. Phys.* **1999**, *111*, 1096−1103.

(14) Obst, S.; Bradaczek, H. *J. Phys. Chem.* **1996**, *100*, 15677−15687.

(15) Schwenk, C. F.; Loeffler, H.; Rode, B. *Chem. Phys. Lett.* **2001**, *349*, 99−103.

(16) Bakó, I.; Hutter, J.; Pálinkás, G. *J. Chem. Phys.* **2002**, *117*, 9838−9843.

(17) Merrill, G. N.; Webb, S.; Bivin, D. *J. Phys. Chem. A* **2003**, *107*, 386−396.

(18) Sprik, M.; Impey, R. W.; Klein, M. L. *Phys. Rev. Lett.* **1986**, *56*, 2326−2329.

(19) Martyna, G. J.; Klein, M. L. *J. Chem. Phys.* **1992**, *96*, 7662−7671.

(20) Mundy, C. J.; Kuo, I.-F. W. *Chem. Rev.* **2006**, *106*, 1282−1304.

(21) Tsuchida, E.; Kanada, Y.; Tsukada, M. *Chem. Phys. Lett.* **1999**, *311*, 236−240.

(22) Morrone, J. A.; Tuckerman, M. E. *Chem. Phys. Lett.* **2003**, *370*, 406−411.

(23) Morrone, J. A.; Tuckerman, M. E. *J. Chem. Phys.* **2002**, *117*, 4403−4413.

(24) Handgraaf, J.-W.; Meijer, E. J. *J. Chem. Phys.* **2004**, *121*, 10111−10119.

(25) Pagliai, M.; Cardini, G.; Righini, R.; Schettino, V. *J. Chem. Phys.* **2003**, *119*, 6655−6662.

(26) Handgraaf, J.; van Erp, T.; Meijer, E. *Chem. Phys. Lett.* **2003**, *367*, 617−624.

(27) Haughney, M.; Ferrario, M.; McDonald, I. R. *Mol. Phys.* **1986**, *88*, 849−853.

(28) Haughney, M.; Ferrario, M.; McDonald, I. R. *J. Phys. Chem.* **1987**, *91*, 4934−4940.

(29) Jorgensen, W. L. *J. Am. Chem. Soc.* **1980**, *102*, 543−549.

(30) Pagliai, M.; Cardini, G.; Schettino, V. *J. Phys. Chem. B* **2005**, *109*, 7475−7481.

(31) Faralli, C.; Pagliai, M.; Cardini, G.; Schettino, V. *Theor. Chem. Acc.* **2007**, *118*, 417−423.

(32) Impey, R. W.; Sprik, M.; Klein, M. L. *J. Am. Chem. Soc.* **1987**, *109*, 5900−5904.

(33) Jorgensen, W. L.; Bigot, B.; Chandrasekhar, J. *J. Am. Chem. Soc.* **1982**, *104*, 4584−4591.

(34) Chandrasekhar, J.; Jorgensen, W. L. *J. Chem. Phys.* **1982**, *77*, 5080−5089.

(35) Sesé, G.; Padró, J. A. *J. Chem. Phys.* **1998**, *108*, 6347−6352.

(36) Islam, M. S.; Pethrick, R. A.; Pugh, D. *J. Phys. Chem. A* **1998**, *102*, 2201−2208.

(37) Masella, M.; Cuniasse, P. *J. Chem. Phys.* **2003**, *113*, 1866−1873.

(38) Narayanan, S.; Gottesfelf, S.; Zawodzinski, T. *Direct Methanol Fuel Cells*; Electrochemical Society: November 2001.

(39) Whitacre, J.; Valdez, T.; Narayanan, S. *J. Electrochem. Soc.* **2005**, *152*, A1780−A1789.

(40) Seo, M.; Yun, Y.; Lee, J.; Tak, Y. *J. Power Sources* **2006**, *159*, 59−62.

(41) Yang, Y.; Liang, Y. C. *J. Power Sources* **2007**, *165*, 185−195.

(42) Wang, Z.; Yin, G.; Shao, Y.; Yang, B.; Shi, P.; Feng, P. *J. Power Sources* **2007**, *165*, 9−15.

(43) *CPMD V 3.9 Copyright IBM Corp 1990−2004*; Copyright MPI für Festkörperforschung: Stuttgart, Germany, 1997−2001.

(44) Car, R.; Parrinello, M. *Phys. Rev. Lett.* **1985**, *55*, 2471−2474.

(45) Tse, J. S. *Ann. Rev. Phys. Chem.* **2002**, *53*, 249−290.

(46) Hutter, J.; Iannuzzi, M. *Z. Kristallogr.* **2005**, *220*, 549−551.

(47) White, J.; Schwegler, E.; Galli, G.; Gygi, F. *J. Chem. Phys.* **2000**, *113*, 4668−4673.

(48) Ikeda, T.; Hirata, M.; Kimura, T. *J. Chem. Phys.* **2003**, *119*, 12386−12392.

(49) Ramaniah, L. M.; Bernasconi, M.; Parrinello, M. *J. Chem. Phys.* **1999**, *111*, 1587−1591.

(50) Lightstone, F. C.; Schwegler, E.; Hood, R. Q.; Gygi, F.; Galli, G. *Chem. Phys. Lett.* **2001**, *343*, 549−555.

(51) Marx, D.; Sprik, M.; Parrinello, M. *Chem. Phys. Lett.* **1997**, *273*, 360−366.

(52) Naor, M. M.; Nostrand, K. V.; Dellago, C. *Chem. Phys. Lett.* **2003**, *369*, 159−164.

(53) Blumbergerer, J.; Sprik, M. *J. Phys. Chem. B* **2004**, *108*, 6529−6535.

(54) Blumberger, J.; Bernasconi, L.; Tavernelli, I.; Vuilleumier, R.; Sprik, M. *J. Am. Chem. Soc.* **2004**, *126*, 3928−3938.

(55) Lyubartsev, A. P.; Laasonen, K.; Laaksonen, A. *J. Chem. Phys.* **2001**, *114*, 3120−3126.

(56) Vuilleumier, R.; Sprik, M. *J. Chem. Phys.* **115**, *8*, 3454−3468.

(57) Tuckerman, M.; Laasonen, K.; Sprik, M.; Parrinello, M. *J. Chem. Phys.* **1995**, *103*, 150−161.

(58) Faralli, C.; Pagliai, M.; Cardini, G.; Schettino, V. *J. Phys. Chem. B* **2006**, *110*, 14923−14928.

(59) Krekeler, C.; Delle Site, L. *J. Phys.: Condens. Matter* **2007**, *19*, 192101.

(60) Jorgensen, W. L. *J. Phys. Chem.* **1986**, *90*, 1276−1284.

(61) Becke, A. D. *Phys. Rev. A* **1988**, *38*, 3098−3100.

(62) Lee, C.; Yang, W.; Parr, R. G. *Phys. Rev. B* **1988**, *37*, 785−789.

(63) Troullier, N.; Martins, J. *Phys. Rev. B* **1991**, *43*, 1993−2006.

(64) Kleinman, L.; Bylander, D. M. *Phys. Rev. Lett.* **1982**, *48*, 1425−1428.

(65) Goedecker, S.; Teter, M.; Hutter, J. *Phys. Rev. B* **1996**, *54*, 1703−1710.

(66) Hartwigsen, C.; Goedecker, S.; Hutter, J. *Phys. Rev. B* **1998**, *58*, 3641−3662.

(67) Mercero, J.; Mujika, J.; Matxain, J.; Lopez, X.; Ulgade, J. *Chem. Phys.* **2003**, *295*, 175−184.

(68) Dudev, T.; Lim, C. *J. Phys. Chem. A* **1999**, *103*, 8093−8100.

(69) Bader, R. F. W. *Atoms in Molecules - A Quantum Theory*; Oxford University Press: Oxford, U.K., 1990.

(70) Bader, R. F. W. *Chem. Rev.* **1991**, *91*, 893−928.

(71) Szefczyk, B.; Sokalski, W. A.; Leszczynski, J. *J. Chem. Phys.* **2002**, *117*, 6952−6958.

(72) Marzari, N.; Vanderbilt, D. *Phys. Rev. B* **1997**, *56*, 12847−12862.

(73) Silvestrelli, P. L.; Marzari, N.; Vanderbilt, D.; Parrinello, M. *Solid State Commun.* **1998**, *107*, 7−11.

(74) Radnai, T.; Kálmán, E.; Pollmer, K. *Z. Naturforsch., A: Phys. Sci.* **1984**, *39A*, 464−470.

(75) Tamura, Y.; Spohr, E.; Heinzinger, K.; Pálinkás, G.; Bakó, I. *Ber. Bunsenges Phys. Chem.* **1992**, *96*, 147−158.

(76) Megyes, T.; Grósz, T.; Radnai, T.; Bakó, I.; Pálinkás, G. *J. Phys. Chem. A* **2004**, *108*, 7261−7271.

(77) Megyes, T.; Bálint, S.; I. Bakó, T. G.; Radnai, T.; Pálinkás, G. *Chem. Phys.* **2006**, *327*, 415−426.

(78) Raugei, S.; Klein, M. L. *J. Chem. Phys.* **2002**, *116*, 196−202.

(79) Ohtaki, H.; Radnai, T. *Chem. Rev.* **1993**, *93*, 1157−1204.

(80) Richens, D. T. *The Chemistry of Aqua Ions*; Wiley: 1997.

(81) Masia, M.; Rey, R. *J. Chem. Phys.* **2005**, *122*, 094502.

(82) Jiao, D.; King, C.; Grossfield, A.; Darden, T.; Ren, P. *J. Phys. Chem. B* **2006**, *110*, 18553−18559.

(83) Svishchev, I. M.; Kusalik, P. G. *J. Chem. Phys.* **1993**, *99*, 3049−3058.

(84) Svishchev, I. M.; Kusalik, P. G. *J. Chem. Phys.* **1994**, *100*, 5165−5171.

(85) Khalack, J. M.; Lyubartsev, A. P. *J. Chem. Phys.* **2005**, *109*, 378−386.

(86) De la Peña, L. H.; Kusalik, P. *J. Am. Chem. Soc.* **2005**, *127*, 5246−5251.

(87) Ikeda, T.; Boero, M.; Terakura, K. *J. Chem. Phys.* **2007**, *126*, 034501.

(88) Lightstone, F. C.; Schwegler, E.; Allesch, M.; Gygi, F.; Galli, G. *Chem. Phys. Chem.* **2005**, *6*, 1745−1749.

(89) Sun, W.; Chen, Z.; Huang, S.-Y. *Fluid Phase Equilib.* **2005**, *238*, 20−25.

(90) Suresh, S. J.; Prabhu, A.; Arora, A. *J. Chem. Phys.* **2007**, *126*, 134502.

(91) Marx, D.; Heinzinger, K.; Pálinkás, G.; Bakó, I. *Z. Naturforsch., A: Phys. Sci.* **1991**, *46A*, 887−897.

(92) Palinkas, G.; Heinzinger, K. *ACH - Models Chem.* **1995**, *132*, 5−29.

(93) Tongraar, A.; Liedl, K.; Rode, B. *J. Phys. Chem. A* **1998**, *102*, 10340−10347.

(94) Brodskaya, E.; Lyubartsev, A. P.; Laaksonen, A. *J. Chem. Phys.* **2006**, *116*, 7879−7892.

(95) Tongraar, A.; Rode, B. *Chem. Phys. Lett.* **2001**, *346*, 485−491.

(96) Parr, R. G.; Pearson, R. G. *J. Am. Chem. Soc.* **1983**, *105*, 7512−7516.

(97) Shannon, R. D.; Prewitt, C. *Acta Crystallogr., Sect. B: Struct. Sci.* **1969**, *B25*, 925−946.

(98) Shannon, R. D. *Acta Crystallogr., Sect. A: Found. Crystallogr.* **1976**, *A32*, 751−767.

(99) Fuentealba, P.; Parr, R. G. *J. Chem. Phys.* **1991**, *94*, 5559−5564.

(100) Ghanty, T.; Ghosh, S. *J. Phys. Chem.* **1994**, *98*, 9197−9201.

CT700209V